

**AJK2015-140655**

## **NUMERICAL SIMULATION OF HEAT TRANSFER TO OPTIMIZE DNA AMPLIFICATION IN POLYMERASE CHAIN REACTION**

**Rabia Jamshaid**

NUST College of Electrical & Mechanical  
Engineering, National University of Sciences &  
Technology, Islamabad, Pakistan 46000

**Tahir Zaidi**

NUST College of Electrical & Mechanical  
Engineering, National University of Sciences &  
Technology, Islamabad, Pakistan 46000

**Imran Aziz**

NUST College of Electrical & Mechanical  
Engineering, National University of Sciences &  
Technology, Islamabad, Pakistan 46000

**Imran Akhtar**

NUST College of Electrical & Mechanical  
Engineering, National University of Sciences &  
Technology, Islamabad, Pakistan 46000

### **ABSTRACT**

Polymerase Chain Reaction (PCR) is a biomedical technique for forensic laboratory sciences in which small amount of DNA is amplified through repeated thermal cycles. It has become a powerful technique for clinical, biological, medical, forensic and genetic analysis and other areas of life science. This process actively increases the quantity of DNA by repetition of three-step procedure i.e. denaturation, annealing and extension which are performed at 95°C, 55°C and 72°C respectively. The temperature sensitivity of the reaction requires precise temperature control and proper thermal isolation of these three zones. In this paper, a three-dimensional heat transfer simulation of a continuous flow based PCR model is performed to study the effect of heat transfer on temperature distribution and thermal gradients in the PCR device. For improving the computational time, one pass simulation model is used. Heaters of 8mm and 9mm lengths are used to apply isothermal boundary conditions in the reaction zones. In order to improve the temperature uniformity in the extension zone, airgaps of 0.5mm, 1mm and 1.5mm are introduced in the glass substrate. It has been observed that airgaps improves temperature uniformity in the extension zone of PCR channel. The effect of heat loss via convection is also observed and it is shown thermal isolation of glass domain from outside improves the temperature distribution in the reaction zones. ANSYS CFX 14 is used to perform Computational fluid dynamics (CFD) simulations by varying the velocity to analyze the effect of fluid convection on the temperature distribution in the channel and to

calculate the residence time of the fluid to attain efficient DNA amplification.

*Keywords:* Polymarase chain reaction (PCR), DNA amplification, Computational fluid dynamics (CFD)

### **INTRODUCTION**

Polymerase chain reaction (PCR) is an enzymatic strategy for the amplification of nucleic acid that is needed to store and interpret hereditary data. It has been used in wide range of applications for clinical, medical diagnostic, biological, forensic and genetic analysis and other areas of life science. The PCR microfluidic devices took great pace in the last two decades when the lab on a chip concept was developed for clinical and biomedical analysis. This process significantly enhance the initial low amount of DNA to an extent that a single target DNA molecule can be amplified up to  $10^6$  molecules [1]. The PCR assays are classified into isothermal, two and three step PCR process [2-3]. In a three-step PCR process, the amplification of a DNA strand is performed in three principle steps [4] namely, denaturation, annealing and extension. In the denaturation step, the original double stranded DNA splits into two single-stranded DNA-molecules (ssDNA) through heating or radiation. This denaturation or melting of DNA occurs at temperatures of about 90-95 °C. In the annealing step, temperature is lowered to about 50-55 °C so that the small complementary DNA-molecules (so-called primers) attach themselves to their defined sites of the single - strand DNA molecules. In extension step, the polymerase molecules bind themselves to the single-strand DNA,

complementary DNA strand is formed, leading finally to an identical copy of the original double-stranded DNA at about 65-75 °C [4]. These three steps are shown in Fig. 1.

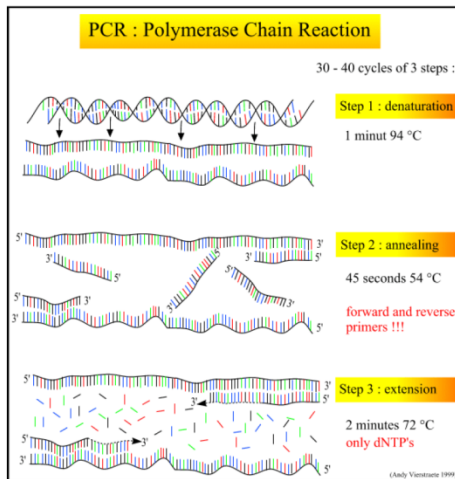


**FIGURE 1: PCR STEPS [4]**

Now days, Miniaturized PCR based biochip has become achievable due to improvements in MEMS technology. The current PCR chip designs can be classified into two groups: chamber based PCR and continuous flow PCR (CFPCR). In the continuous flow PCR, the solution is continuously and repeatedly moved through the three different fixed temperature zones, which are essential for PCR multiplication. So, the possibilities of cross contamination between different experiments are reduced, less energy consumption and fast heating and cooling rates are achieved as only the flowing fluid has to be heated instead of entire chip. In 1994, Nakano et al. [5] for the developed first time novel capillary-based CFPCR whose reaction time was completed in 12 to 18 minutes. Kopp et al. [6] developed the first CFPCR chip in 1998. The chip was developed using Corning 0211 glass with channels width and depth of 90  $\mu\text{m}$  and 40  $\mu\text{m}$ , respectively. Chip was attached on three copper pieces that were heated by three capsule heaters. The PCR reaction mixture was pushed through a channel and moved between the three heating zones. Schneegaß et al. [7] presented CFPCR chip made of silicon and glass that could be used for the amplification of various DNA templates of different sources. The individual temperature zones were insulated by etching airgaps on the wafers. A cooling block was connected in the annealing zone to avoid overheating from the adjacent temperature zones. Hashimoto et al. [8] analyzed the performance of a spiral type CFPCR device in which thermal insulation was done by milling air pockets above and below the microchannels. Wang et al. [9] fabricated a droplet-based micro oscillating-flow PCR chip. The pressure generated from an injector drove a microliter-sized droplet. The droplet flew through three sequential temperature zones back and forth. The electrophoresis results showed that the chip successfully amplified the HPV DNA within 15 min.

Yao et al. [10] used excimer laser to fabricate a poly methyl methacrylate (PMMA) based CFPCR chip. The heating source was electric thin film which was separated from the channel by a copper flake to maintain the uniform temperature distribution between reaction zones of the chip. Shih et al. [11] utilized a parylene-cross-linking structure to achieve on-chip airgap thermal isolation for the CFPCR chip. Results showed that a 10-cycle PCR chip was prepared on an 8 mm×8 mm silicon chip area among three temperature zones. Kim et al. [12] presented a device with three thermoelectric module heaters to control the three heating temperatures. The width of each temperature zone was about 15.5 mm. Due to the size limitation of the Peltier cooling and the thermoelectric heating modules, the width of the temperature zone of the PCR chip with thermoelectric modules was larger than 15 mm. Chen et al. [13] used LIGA technology to fabricate a polycarbonate CRPCR device. They made small grooves to increase the resistance to heat conduction between the three temperature zones. Fang et al. [14] used three external thermoelectric heaters for three temperature zones of the PCR process. The overall dimension of their chip was 55 mm× 83 mm, the width of each temperature zone was about 18 mm. Zhang and Xing [15] optimized the annealing temperature parameter for the PCR performance within the microfluidic device. The PCR performed well within the annealing temperatures ranging from 333 K to 341 K. Manage et al. [16] used the unprocessed whole blood for genomic targets amplified by PCR on a microfluidic chip. Three valves were used to pump the reagents from the loading well to the sample reservoir. Li et al. [17] designed capillary-based CFPCR device, which used flexible thin film heaters to construct three temperature zones. The temperature uniformity was improved by applying a brass sheet onto the surface of thin film heater. Xue et al. [18] developed an intelligent temperature control circuit, performed experiment and FEA simulations. Kumar et al. [19-20] used periodic boundary conditions to simulate the whole channel using a single cycle; they discovered that single cycle is good enough for simulating the whole model.

This study employs a PCR channel in which extension zone lies in the middle of channel with 5 turns with denaturation and annealing zones on the either side of it. Three dimensional heat transfer simulations are performed using commercial finite volume based software ANSYS CFX 14 [21]. Various configurations of heaters are used to analyze their effect on heat transfer in the channel. At first, three heaters of 8mm width are used with and without airgaps. Simulations are repeated using 9mm width heater with and without air gaps. We then studied the effect of adiabatic boundary conditions on temperature distribution in the channel. After achieving optimum configuration according to the avoidance of thermal cross talk and heater width effect, the final set up is analyzed with different flow velocities to observe the impact of fluid velocity on temperature distribution in the channel. Finally, residence time at different velocities is analyzed in order to attain optimum time for efficient DNA amplification.

## CHANNEL DESIGN

PCR device presented in the paper consists of three NiCr heaters, a glass substrate on which the serpentine PCR channel is etched and a glass cover is applied on top of it. The PCR channel consists of 18 cycles with each cycle containing denaturation, annealing and extensions zones at temperatures 95°C, 55°C and 72°C, respectively. The length of entire channel is approximately 1.9m. The NiCr thin film heaters of 8mm and 9mm lateral dimensions are attached to the bottom of the one cycle model. Air gaps of 0.5mm, 1mm and 1.5mm are created to maintain uniform temperatures in the process zones. The channel width is 120 $\mu$ m and height is 30 $\mu$ m. The exploded view of PCR device assembly is presented in Fig. 2.

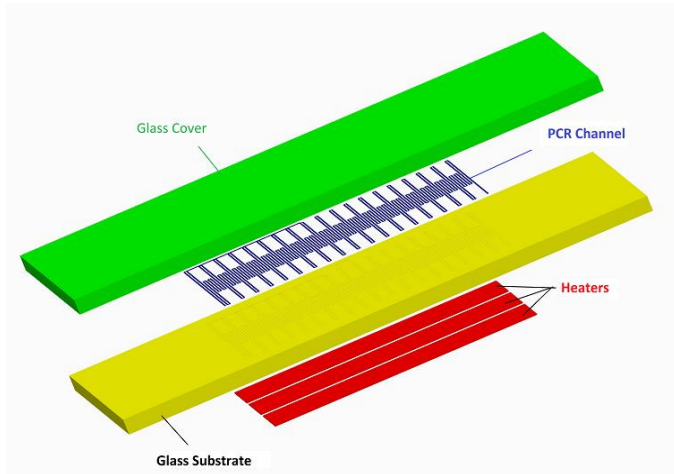


**FIGURE 2: EXPLODED VIEW OF THE PCR DEVICE ASSEMBLY**

The material properties of glass, NiCr heaters and silane are presented in Table 1.

**Table 1: MATERIAL PROPERTIES**

Material Property	Glass	NiCr	Silane
Thermal conductivity(W/m.K)	0.930	11.3	0.59
Specific heat capacity (J/kg.K)	880	450	4175
Density (kg/m <sup>3</sup> )	2530	8400	1005
Dynamic viscosity (pa.s)			8.9e-4

For heat transfer through convection with atmosphere the heat convective coefficient is taken as 6.5 W/m<sup>2</sup>K [22].

The heat transfer in the whole PCR device can be simulated using one pass simulation model by applying periodic boundary conditions [19-20]. We have made a one cycle simulation model as presented in Fig. 3 which shows one-cycle with different zones and dimensions. The length ratios of denaturation, extension and annealing are 1:2:1.

After designing, the one pass configuration of PCR channel is meshed using a hybrid-meshing scheme. PCR channel is meshed using 133326 hexahedral elements. The

glass domain is meshed using 4909548 tetrahedral elements and the three heater zones are meshed using approximately 33300 hexahedral elements. Overall, approximately 5.1 million mesh elements are created. The meshing of the whole one pass configuration is presented in Fig. 4.

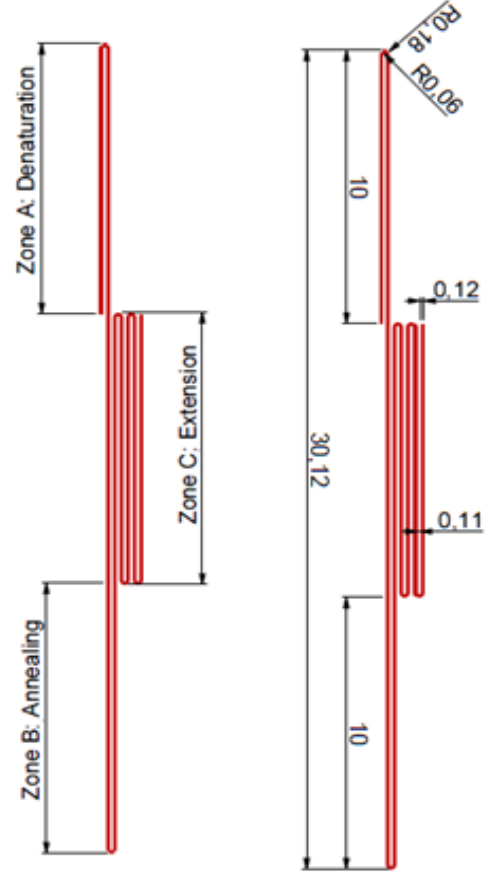


**FIGURE 3: PCR CONFIGURATION AND ONE-CYCLE CHANNEL DIMENSIONS.**

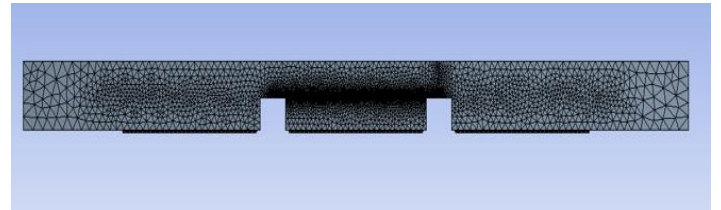
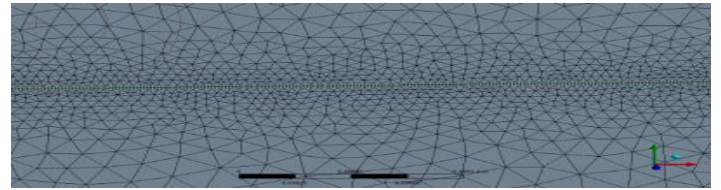


**FIGURE 4: TOP AND SIDE VIEWS OF THE GENERATED MESH.**

## NUMERICAL METHODOLOGY

The velocities of the fluid in continuous flow PCR chips are usually of the order of mm/sec. Because of low velocity, the viscous effects are usually dominant over inertial effects and the Reynolds number determines the flow pattern and is defined as.

$$Re = \frac{\rho v L}{\mu} \quad (1)$$

where  $\rho$  is density of fluid,  $v$  is velocity of fluid,  $L$  is characteristics length of the channel (channel width or depth) and  $\mu$  is the dynamic viscosity. In the present study, the velocity magnitudes considered are in the range of 0.5 mm/sec to 10 mm/sec. Corresponding Reynolds number, therefore, is in the range of 0.027-0.54 and lie in the laminar regime. Pressure drop calculated analytically for the whole channel is in the range of 5psi to 9psi.

The incompressible Navier-Stokes equations are the governing equations for the problem and are represented as

$$\frac{\partial \rho}{\partial t} = -\nabla \cdot (\rho v) \quad (2)$$

$$\rho \left( \frac{\partial v}{\partial t} + (v \cdot \nabla) v \right) = \mu \nabla^2 v - \nabla P \quad (3)$$

$$\rho C_p \left( \frac{\partial T}{\partial t} + v \cdot \nabla T \right) = k \nabla^2 T + \tau \cdot \nabla v \quad (4)$$

where  $v$  is velocity vector,  $C_p$  is the heat specific capacity,  $T$  is temperature,  $\tau$  is the viscous shear stress and  $k$  is thermal conductivity.

The three dimensional energy transfers in the PCR chip is governed by the steady state heat equation as

$$\frac{\partial^2 T}{\partial x^2} + \frac{\partial^2 T}{\partial y^2} + \frac{\partial^2 T}{\partial z^2} = 0 \quad (5)$$

## BOUNDARY CONDITIONS:

The selection of boundary conditions is necessary for getting the correct results for the problem. For fluid flow, we use velocity as an inlet boundary condition and zero static pressure is used at the outlet. In order to study the effect of convection on the temperature and to compute residence time we vary the velocity at inlet in the range of 0.5mm/sec to 10mm/sec. Isothermal boundary conditions of 368K, 346K, and 328K are used for the three heaters to provide constant temperatures for denaturation, annealing, and extension zones respectively. Convective boundary conditions are applied at the top and sidewalls of the glass domain with convection heat transfer coefficient of 6.5 W/m<sup>2</sup>K. To see the effect of insulation on the temperature distribution in the fluid channel; adiabatic boundary conditions are used at the top and sides of

the glass domain. One pass simulation model with boundary conditions is presented in Fig. 5.

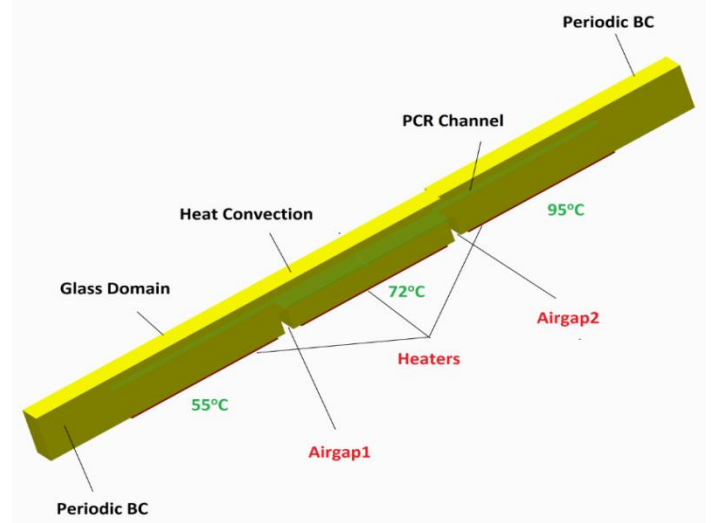


**FIGURE 5: ONE CYCLE SIMULATION MODEL WITH BOUNDARY CONDITIONS.**

## RESULTS AND DISCUSSIONS:

In this work, effect of heater dimensions and air gaps on heat transfer in the fluid domain was studied in order to obtain uniform temperature distribution for specific configuration of our serpentine channel. After the optimization of temperature distribution across the channel, the effects of change in fluid velocity or fluid convection on temperature distribution in the PCR channel is observed.

Three-dimensional heat transfer simulation with heater lateral lengths of 8mm and 9mm shows that the temperature distribution at the ends of the middle extension zone contain large thermal gradients due to heat transfer from denaturation and annealing zones via conduction. The temperatures in the extension zone with no gap are observed to be in the range of 338-355K. To avoid this thermal cross talk in the channel, airgaps of 0.5mm, 1mm and 1.5mm are introduced in the PCR device. This result in improved temperature uniformity in the extension zone and the temperatures range becomes 340-352K. The size of the airgaps has small effect on uniformity, as the temperature distribution in all zones for all size of airgaps varied with a relative temperature variation of <2K. A comparison of temperature distribution along with the channel length with various airgaps configurations for 8mm and 9mm heater configurations is presented in Fig. 6 and Fig. 7.

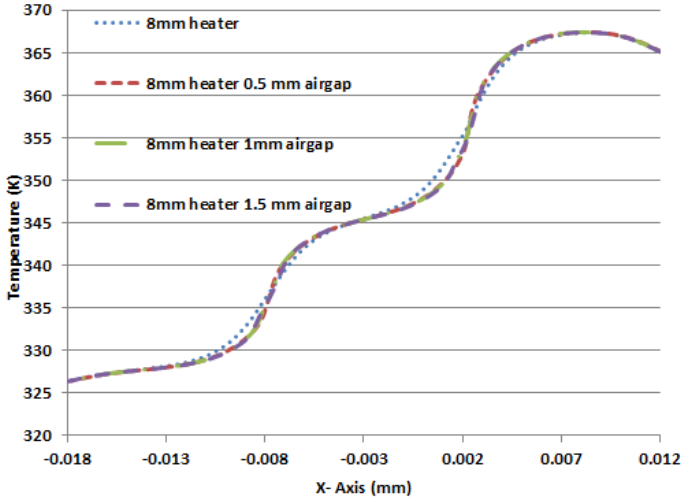


**FIGURE 6:** A COMPARISON OF TEMPERATURE DISTRIBUTION ALONG LATERAL DIRECTION WITH VARIOUS AIRGAPS CONFIGURATIONS FOR 9MM HEATER.

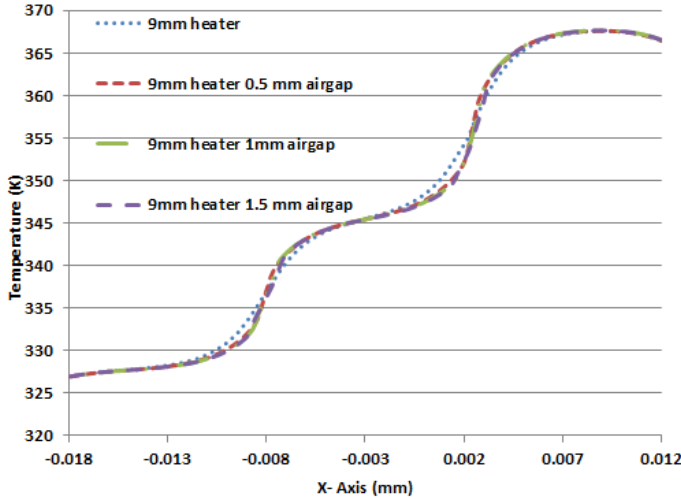


**FIGURE 7:** A COMPARISON OF TEMPERATURE DISTRIBUTION ALONG LATERAL DIRECTION WITH VARIOUS AIRGAPS CONFIGURATIONS FOR 9MM HEATER.

In order to analyze the effect of heater dimension on temperature distribution, the 8mm and 9mm heater configurations with 1mm airgaps are compared in Fig. 8. It is observed 9mm heater provides a more uniform distribution in the extension zone with the improvement of approximately 1K at each end. The increase in length also gives better temperature distribution in the denaturation and annealing zones by a difference of 2K and 1K, respectively.

In addition to this effect of insulation on the top surface of the PCR device and temperature distribution in the PCR channel zones is also studied. It is observed that the dip in temperature profile due to convection in all zones disappears with the application of adiabatic boundary condition at the top surface. This is because the heat loss occurred due to heat transfer to atmosphere via convection. Since the thermal conductivity of glass is low, the convection phenomenon is dominant.

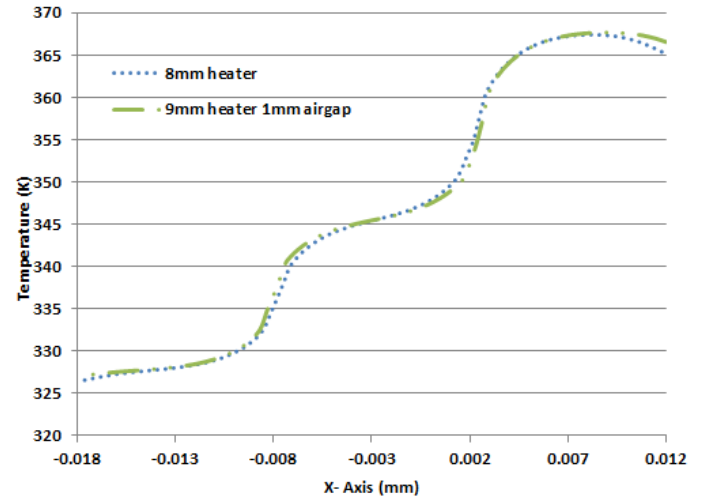


**FIGURE 8:** EFFECT OF HEATERS LENGTH ON THE TEMPERATURE DISTRIBUTION IN DIFFERENT ZONES OF THE PCR CHANNEL.

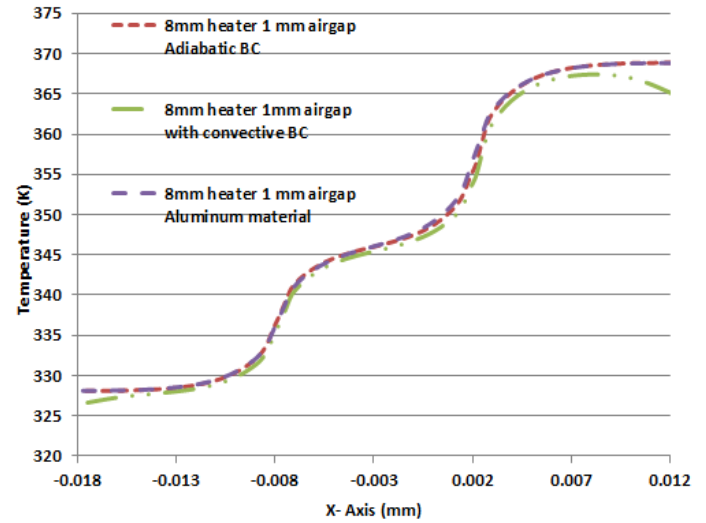


**FIGURE 9:** EFFECT OF ADIABATIC AND CONVECTIVE BOUNDARY CONDITIONS ON THE TEMPERATURE DISTRIBUTION IN THE PCR CHANNEL.

The top surface convection dominance due to low thermal conductivity of glass is vindicated via numerical experimentation by using aluminum as the device material. Similar convective boundary condition at the top and side walls of the channel is applied. Temperature distribution in the fluid domain is similar as observed in with the adiabatic boundary condition. This is due to very high thermal conductivity of aluminum. Comparison of results is presented in Fig. 9. Therefore, in order to prevent heat loss due to convection and save power, an insulation layer on the top surface of PCR device is recommended which will lead to a uniform temperature distribution in a PCR channel.

Based on the present simulations, the 9mm heater configuration with 1mm airgap is chosen to perform further



simulations to investigate the temperature distribution in the transverse direction and along the height of the fluid channel and also to evaluate the effect of varying velocity on temperature distribution in the fluid channel. From Fig. 10 the temperature variations in the transverse direction (neglecting end effects) are found to be small, i.e. less than 1K. As the transverse temperature gradients are much smaller than the temperature gradients in the direction of flow (between heater regions), variations in temperature profiles between different passes as a function of chip position are assumed to be negligible.

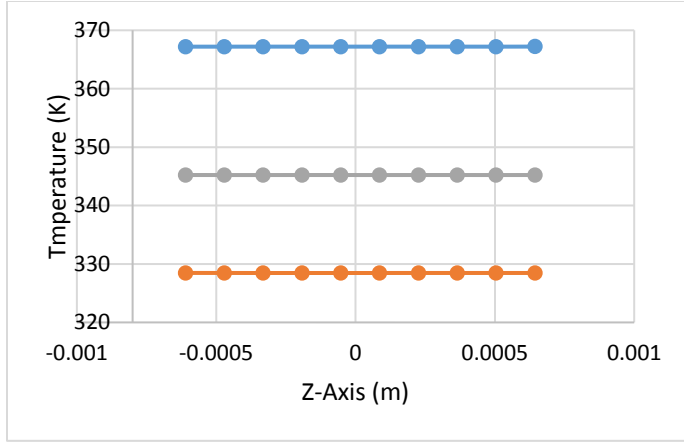


**FIGURE 10:** TEMPERATURE DISTRIBUTION IN TRANSVERSE DIRECTION

Steady state temperature profiles in the fluid domain and in glass domain along the height of the PCR device and along the transverse direction are shown in Fig. 11. As conduction is the dominant mode of heat transfer in the fluid regime, there is little variation in temperature along the height of the fluidic channel (<1K).

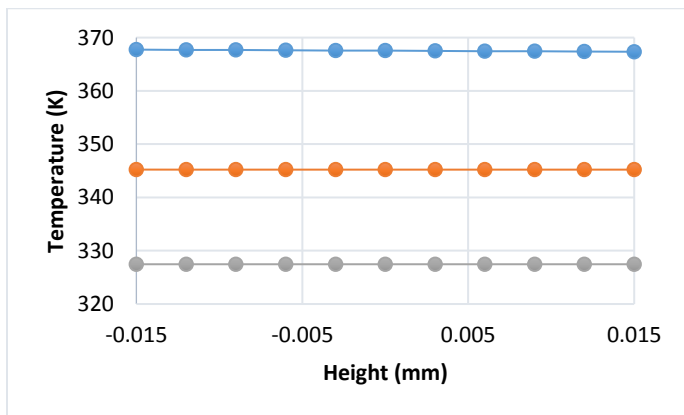


**FIGURE 11:** TEMPERATURE DISTRIBUTION ALONG THE CHANNEL HEIGHT

Further simulations are performed by varying the inlet velocity in the range 0.5 mm/sec to 10 mm/sec or  $1.8 \text{ nl/sec} \leq Q$

$\leq 36 \text{ nl/s}$  where  $Q$  is the flow rate. The spatial temperature distribution in the fluid domain at different velocities is shown in Fig. 12. The results show that change in velocity has a negligible effect on the spatial temperature distribution over the defined flow rate range due to the dominance of conduction over convection in the PCR channel.

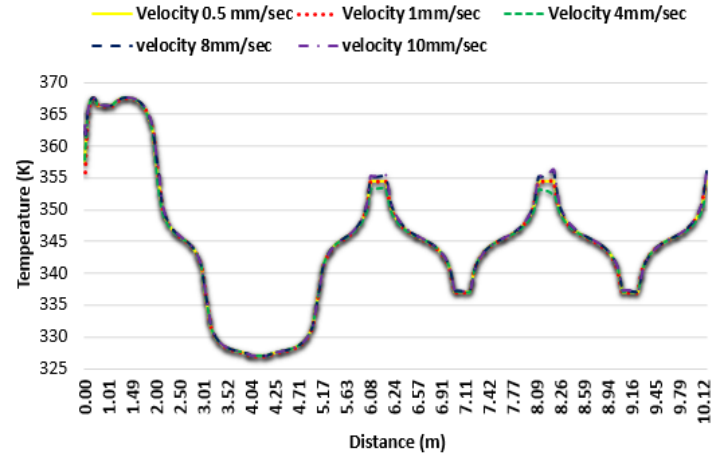


**FIGURE 12:** EFFECT OF VELOCITY ON TEMPERATURE DISTRIBUTION IN THE PCR CHANNEL.

Transient simulations are also performed to compute the residence time for different velocities and is plotted against temperature in Fig. 13. It is analyzed that the residence time of one cycle for velocities in the range 0.5 mm/sec to 10 mm/sec is in the range 10 sec - 205 sec.

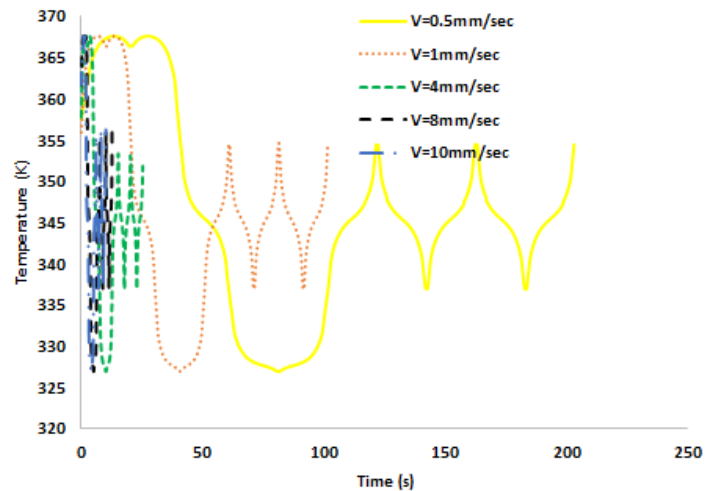


**FIGURE 13:** TEMPERATURE DISTRIBUTION VS RESIDENCE TIME

We choose 4mm/sec as the optimum velocity as it provides sufficient time for denaturation, extension, and annealing processes to occur. The time computed for 0.5mm/sec and 1mm/sec is slow to be termed as optimum time

for DNA amplification. The velocities of 8mm/sec to 10mm/sec give small value of residence time which is not good enough for DNA amplification. It is therefore concluded that for length ratio of 1:2:1, flow rates of 10-15 nl/sec is optimum for efficient DNA amplification.

## CONCLUSIONS:

In this study, three dimensional heat transfer simulation is performed on one pass channel configuration of the PCR device for various configurations of airgaps and heaters. Results show that temperature uniformity in the extension zone improved with addition of airgaps. Size of the airgaps has negligible effect on uniformity, as temperature distribution in all zones for all size of airgaps remained the same. It is observed that 9mm heater provides a more uniform distribution in the extension zone with the improvement of approximately 2K at both ends. The increase in length also gives better temperature distribution in the denaturation and annealing zones by a difference of 2K and 1K respectively. In order to prevent heat loss due to convection and save power, an insulation on top surface of the PCR device is recommended which will lead to a uniform temperature distribution in a PCR channel. Temperature distribution in the transverse direction and along with the height of the channel was uniform. Further results showed that change in volume flow rate has a negligible effect on spatial temperature distribution over the defined flow rate range due to the dominance of conduction over convection. The study provides useful knowledge of the effect of heater dimensions and airgaps on the thermal profile of the proposed PCR device. It is concluded that the flow rate range of 10-15 nl/sec is suitable for efficient DNA amplification.

## REFERENCES

- [1] J. Liu, M. Enzelberger, S. Quake, "A nanoliter rotary device for polymerase chain reaction," *Electrophoresis*, vol. 23, pp. 1531–1536, 2002.
- [2] C. C. Chang, C. C. Chen, S. H. Wei, H. H. Lu, Y. H. Liang, C. W. Lin, "Diagnostic devices for isothermal nucleic acid amplification," *Sensors*, vol. 12, 8319–8337, 2012.
- [3] W. Rychlik, W. J. Spencer, R. Rhoads, "Optimization of the annealing temperature for DNA amplification in vitro," *Nucleic Acids Res*, vol. 18, pp. 6409–6412, 1990.
- [4] A. Tichopad, "Quantitative real-time RT-PCR based transcriptomics: improvement of evaluation methods," PhD dissertation, Technical University of Munich, Germany, 2004.
- [5] Nakano, H., Matsuda, K., Yohda, M., Nagamune, T., Endo, I. and Yamane, T. (1994). High-speed polymerase chain-reaction in constant flow. *Biosci. Biotechnol. Biochem.* 58, 349–352.
- [6] M.U. Kopp, A.J.D. Mello, A. Manz, 1998. "Chemical amplification: continuous-flow PCR on a chip". *Science* 280, pp. 1046–1048.
- [7] I. Schneegeß, R. Brautigam, J.M. Kohler, 2001. "Miniaturized flow-through PCR with different template types in a silicon chip thermocycler". *Lab Chip*-1, pp. 42–49.
- [8] Masahiko Hashimoto, Pin-Chuan Chen, Michael W. Mitchell, Dimitris E. Nikitopoulos, Steven A. Soper and Michael C. Murphy, 2004. "Rapid PCR in a continuous flow device". *Lab on a Chip*, Volume-4, October, pp. 638–645.
- [9] W. Wang, Z.X. Li, R. Luo, S.H. Lu, A.D. Xu, Y.J. Yang, 2005. "Droplet-based micro oscillating-flow PCR chip". *Journal of Micromechanics and Microengineering*. Volume 15, pp. 1369–1377.
- [10] L. Yao, B. Liu, T. Chen, S. Liu, T. Zuo, 2005. "Micro flow-through PCR in a PMMA chip fabricated by KrF excimer laser". *Biomed. Microdevices* 7, Issue 3, pp. 253–257.
- [11] C.Y. Shih, Y. Chen, Y.C. Tai, 2006. "Parylene-strengthened thermal isolation technology for microfluidic system-on-chip applications". *Sensors Actuators A Phys.* Volume 126, pp. 270–276.
- [12] J.A. Kim, J.Y. Lee, S. Seong, S.H. Cha, S.H. Lee, J.J. Kim, T.H. Park, 2006. "Fabrication and characterization of a PDMS-glass hybrid continuous-flow PCR chip". *Biochemical Engr Journal*. 29, pp. 91–97.
- [13] P.C. Chen, D.E. Nikitopoulos, S.A. Soper, M.C. Murphy, 2008. "Temperature distribution effects on micro-CFPCR performance. *Biomed. Microdevices* 10, pp. 141–152.
- [14] T.H. Fang, N. Ramalingam, D. Xian-Dui, T.S. Ng, Z. Xianting, A.T. Lai Kuan, E.Y. Peng Huat, G. Hai-Qing, 2006. "Real-time PCR microfluidic devices with concurrent electrochemical detection". *Biosensor and Bioelectron.* 24(7), pp. 2131–2136.
- [15] C. Zhang, D. Xing, 2010, "Microfluidic gradient PCR (MG-PCR); a new method for microfluidic DNA amplification", *Biomedical Microdevices*, Vol 12, pp 1–12.
- [16] D.P. Manage, Y.C. Morrissey, A.J. Stickel, J. Lauzon, A. Atrazhev, J.P. Acker, L.M. Pilarski, 2011. "On-chip PCR amplification of genomic and viral templates in unprocessed whole blood". *Microfluid. Nanofluid.* 10, pp. 697–702.
- [17] Y. Li, C. Zhang, D. Xing, 2011. "Fast identification of foodborne pathogenic viruses using continuous-flow reverse transcription-PCR with fluorescence detection". *Microfluid. Nanofluid.* 10, pp. 367–380.
- [18] N. Xue, W. Yan, "Glass-based continuous flow PCR chip with a portable control system for DNA amplification," *IEEE Sensors Journal*, vol. 12, NO. 6, 2012.
- [19] Sumeet Kumar, Todd Thorsen, Sarit Kumar Das, 2008. "Thermal modeling for design optimization of a microfluidic device for continuous flow polymerase chain reaction (PCR)". *Proceedings of ASME Summer Heat Transfer Conference*, August Jacksonville, Florida USA.
- [20] S. Kumar, M. A. C. Ayala, T. Thorsen, "Thermal modeling and design analysis of a continuous flow microfluidic chip," *International Journal of Thermal Sciences*, vol. 67, pp. 72–86, 2013.
- [21] ANSYS, Inc. Release 14.0, South Pointe, 275 Technology Drive, Canonsburg, PA 15317 November 2011.

[22] J. J. Chen, C. M. Shen, and Y. W. i Ko, 2013. “Analytical study of a microfluidic DNA amplification chip using water cooling effect”. *Biomed Microdevices*, 15, pp. 261–278